Characterization of Single Walled Carbon Nanotubes using Comparative Laser Technique

Daniel N. Njoroge

Abstract*: This study was based on characterization of single walled carbon nanotubes (SWNTs) with Raman spectroscopy. The SWNTs samples were subjected to Raman scattering with lasers of 532 nm and 633 nm. The study outlines use of Raman spectroscope, preparation of samples under investigation, obtaining and finally analyzing the Raman spectra. In this study, the samples were prepared for Raman spectroscopy inspection, sampling parameters optimized to obtain good spectra and Raman spectra analyzed. Raman spectroscopy is an important material testing tool. It can be used to sort materials which have been mixed since every material has unique chemical structure which translates to a unique spectrum. Most importantly, it can also be used to identify defects in a sample.

***Index Terms*: Carbon nanotubes, Raman spectroscopy.**

I. INTRODUCTION

Spectroscopy is a subject concerned with the absorption, emission or scattering of electromagnetic radiation by atoms or molecules [1]. When electromagnetic radiation falls on an atomic or molecular sample it is either absorbed, transmitted or scattered. Absorption occurs if energy of radiation corresponds to the separation of two energy levels of atoms or molecules. Most of the scattered radiation is of unchanged wavelength (or wavenumber) and is referred to as Rayleigh scattering or elastic scattering. Part of the scattered radiation is of increased or decreased wavelength (or wavenumber) and is referred to as inelastic scattering or Raman scattering. The scattered radiation with decreased or increased wavenumber corresponds to Stokes and anti-Stokes Raman scattering, respectively [1, 2].

A. Development of Raman Spectroscopy

1930, Raman spectroscopy was only limited to specialised research laboratories [2]. Today, the technique is applied in many applications but there is an increasing chance for misinterpretations of the spectra which can be avoided by good training from Raman spectroscopy experts. Application areas include, research institutions, as a reliable technique for quality control or even for sorting plastics in a recycling industry. Raman spectroscopy technique is a relatively fast method and well-suited to investigating solids, liquids, solutions and even gases, depending on the experimental set-up used. Besides, it has a simple sample preparation procedure hence it is an attractive technique even for new users.

B. Raman Scattering Process

In Raman spectroscopy, an intense, monochromatic beam of electromagnetic radiation (usually a laser) is focused on the sample, and the intensity of the scattered radiation is measured as a function of its wavelength. Usually, in a Raman spectrum the intensity is plotted as a function of the Raman wavenumber (ω), expressed in cm^{-1}. Raman wavenumber (ω), is related to the difference in frequency between the scattered light and the incident electromagnetic radiation according to (1);

$$\omega = \frac{v_m}{c} = \frac{v_o}{c} \qquad (1)$$

Where (v_m) is the frequency of scattered radiation, (v_o) is the frequency of incident radiation and c is the speed of light [2].

C. Selection Rule

When a molecule is positioned in an electric field, E an electric dipole moment, P is induced according to (2);

$$P = \alpha E + \frac{1}{2}\beta E^2 + \frac{1}{6}\gamma E^3 + \cdots \qquad (2)$$

Where α is the polarisability tensor, β the hyper-polarisability tensor and γ the second hyper-polarisability tensor. Neglecting higher orders of the power series, (2) can be reduced to (3);

$$P = \alpha E \qquad (3)$$

Where electric dipole moment, P is directly related to the electric field, E. Polarisability tensor, α depends on the shape and dimensions of the chemical bond. Since the chemical bonds change during vibration, α is thus dependent on the vibrations of the molecule [2]. Therefore, for Raman scattering to occur, a change in polarisability must occur i.e polarisability derivative to the normal coordinate, Q under equilibrium conditions should be non-zero as shown in (4).

$$\alpha' = \frac{\partial \alpha}{\partial Q} \neq 0 \qquad (4)$$

D. Vibration Modes of Molecules

There are several normal vibrational modes of molecules namely; symmetric stretching, asymmetric stretching and bending vibrations. Vibration modes that are Raman active, are infrared inactive and vice-versa.

Revised Version Manuscript Received on March 06, 2017.

Daniel N. Njoroge, Department of Mechanical and Manufacturing Engineering, Aalborg University, Fibigerstraede 16, DK-9220 Aalborg East, Denmark, E-mail: daniel.nyumu@gmail.com

During a symmetric stretch, the polarisability of the molecule changes, but the dipole moment does not change, hence the vibration is Raman active. In asymmetric stretch, the dipole moment of the molecule changes but not the polarisability, hence the vibration is infrared active. Finally, during a bending vibration, the dipole moment of the molecule changes but not the polarisability, hence the vibration is infrared active. Stretch vibrations occur at higher wavenumbers than bending vibrations. This is because, stretch vibrations involve bond length changes, whereas bending vibrations are bond angle changes. In principle changing a bond length requires more energy than changing a bond angle.

E. Position of the Raman Band

The overall energy difference, E_k for Raman transitions, from one energy level to the next, of vibrating molecules is represented by (5);

$$E_k = \pm h v_k \tag{5}$$

Where h is the plank's constant and v_k is the molecular vibrational frequency. In Raman scattering, vibration of molecules is considered as a harmonic oscillation according to (6);

$$v_k = \frac{1}{2\pi}\sqrt{\frac{k}{\mu}} \tag{6}$$

Where v_k is the vibrational frequency, k is the force constant of bond and μ is the reduced mass. For a diatomic molecule, the reduced mass, μ is given by (7);

$$\frac{1}{\mu} = \frac{1}{m_1} + \frac{1}{m_2} \tag{7}$$

Where m_1 and m_2 are masses of atoms constituting the bond. Equation (7) can be expanded to represent multi-atomic molecules. Analyzing (5), (6) and (7), it can be concluded that k and μ are two factors which determine the Raman band position.

F. Raman Bandwidth

Variation of position of the Raman band in the spectra influences the Raman bandwidth. This is recorded by the variations of the two factors which determine the Raman band position, i.e k and μ. These factors are influenced by the chemical environment and atomic masses respectively. If the bonds present in the measured volume do not have the same chemical environment, there is a range of slightly different $k's$ which subsequently causes band broadening. Due to this effect, Raman bands of amorphous materials are broader than those of crystalline materials. In the case where Raman bands are closer than the spectral resolution of the spectrometer, Raman bands are observed as a single broader band [2].

G. Raman Intensity

The intensity of Raman scattered radiation I_R is given by (8);

$$I_R \propto v^4 I_o N \left(\frac{\partial \alpha}{\partial Q}\right)^2 \tag{8}$$

Where I_o is the incident laser intensity, N the number of scattering molecules in a given state, v the frequency of the exciting laser, α the polarisability of the molecules, and Q the vibrational amplitude [3].

II. EXPERIMENTAL

A. Materials

Single walled carbon nanotubes (SWNTs) were used as received.

B. Characterization

1) Acquisition of Raman spectrum

The Raman spectroscopy measurement was carried out as shown in Fig. 1. The measurements were performed using a dispersive Raman spectroscopy with 532 nm and 633 nm lasers. Typically, the preparation procedure of the spectra measurement was conducted as follows: The computer controlled Raman spectrometer system was switched on and the software launched. The sample was then put under the objective lens, laser selection (500 nm or 633 nm) and focusing of the sample on the surface was achieved through x, y, and z movements of the table where the sample rests. The equipment was then automatically calibrated before any measurements were taken.

To achieve a Raman spectrum, the sample is illuminated with a laser beam. Electromagnetic radiation from the illuminated spot is collected with a lens and sent through a monochromator. Elastic scattered radiation at the wavelength corresponding to the laser line (Rayleigh scattering) is filtered out, while the rest of the collected light is dispersed onto the charge-coupled device (CCD) detector by either a notch filter or a band pass filters.

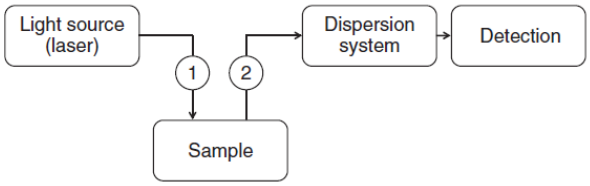

Fig. 1 Raman Spectroscopy. 1 Optics to Focus the Laser Beam on the Sample; 2 Collection Optics for the Scattered Radiation.

C. Baseline correction and Deconvolution

In a Raman spectrum, apart from the Raman bands, other features present are; fluorescence or background radiation. All spectra were baseline corrected and smoothed to reduce the baseline variability and background noises at the region between 550 and 2000 cm^{-1}. The automatic approach was utilized. The curve fitting was done using the Lorentzian fit of the spectra.

III. RESULTS AND DISCUSSION

In this section, spectra for the SWNTs taken from different lasers were analysed and discussed. All spectra were analysed in the same way as outlined above. Comparison of the spectra was also performed to conclude about the diameter ranges of the SWNTs.

Published By:
Blue Eyes Intelligence Engineering
& Sciences Publication Pvt. Ltd.

Three vibration modes were identified in the structure namely: radial breathing mode (RBM), tangential mode (G-Band) and the disorder-induced mode (D-Band).

A. Vibration Modes

1) Radial Breathing Mode (RBM)

RBM is observed in the range 120 - 250 cm^{-1} and corresponds to the atomic vibration of Carbon atoms in the radial direction [4]. RBM was identified in the SWNTs spectra as seen in Fig. 2. The Fig. 2a shows a spectrum from 532 nm laser while Fig. 2b shows a second spectrum using a 633 nm laser. Both spectra were taken in the same range of 100 and 500 cm^{-1}. In both spectra, RBM was more pronounced at 183 cm^{-1} in the 532 nm laser spectrum and at 186 cm^{-1} in the 633 nm laser spectrum. These peaks are RBM from the resonant SWNTs.

2) Tangential mode (G-Band)

G-Band is observed around 1580 cm^{-1} and is seen as multiple peaks in the spectrum [4]. G-Band was identified in the SWNTs spectra as shown in Fig. 3. Fig. 3a shows a spectrum from 532 nm laser while Fig. 3b shows a second spectrum using a 633 nm laser. Both spectra were taken in the same range of 1500 and 1700 cm^{-1}. In both spectra, G-Band was more pronounced at 1587 cm^{-1} in the 532 nm laser spectrum and at 1588 cm^{-1} in the 633 nm laser spectrum. These peaks are G-Band from the resonant SWNTs.

3) Disorder-induced mode (D-Band)

The SWNTs spectra shows signals around 1450 cm^{-1} which corresponds to noisy background in bad resonance. In good resonance, no D-Band is observed in SWNTs spectra [4]. The noise signal was identified in the SWNTs spectra as shown in Fig. 4 and 3b. The Fig. 4 shows a spectrum from 532 nm laser while Fig. 3b shows a second spectrum achieved using 633 nm laser. The analysed spectrum (Fig. 4) was taken in the range of 1200 and 1500 cm^{-1}. In both spectra, noise signals were detected at 1336 cm^{-1} in the 532 nm laser spectrum and around 1400 cm^{-1} in the 633 nm laser spectrum. These peaks represent the noisy background.

B. Defects

Raman spectra can be used for SWNTs characterization of good quality samples. To identify a defective sample, the single and double resonance mechanisms exhibit the same intensity. On the other hand, for a good quality sample, the single resonance process is two orders of magnitude higher in intensity than the double resonance process [4]. The observation of large D-Band peaks compared with the G-peak intensity in SWNTs usually indicates the presence of amorphous carbon [4].

1) Evaluation of Presence of Defects in the Samples

In this experiment, the samples were investigated only by a single resonance process hence there is no basis to report on the presence of defects in the sample. The proper approach to answer this question would have been to acquire spectra using the double and single resonance processes and then compare the magnitudes of the resulting intensities. In this comparison, the sample with a higher intensity ratio given by (9), where the ratio must be > 1 will contain less defects than its counterpart.

$$Intensity\ ratio = \frac{single\ resonance\ intensity}{double\ resonance\ intensity} \quad (9)$$

C. Range of the Diameters of the Single Walled Carbon Nanotubes

SWNTs have varying diameters and chiral angles in samples formed through any preparative method [5].

There are different ways to characterize the diameter distribution in the SWNTs using the rich Raman spectra. One way to characterize the diameter distribution in SWNTs is by using several Raman spectra achieved through different laser lines. The other ways are: utilizing RBM features and use of the G-Band multipeak features which has been reported to be less accurate than the latter [4].

1) Estimating Diameter Distribution with RBM Features

The radial breathing mode (RBM) frequency of SWNTs has a simple monotonic relation given by (10) to tube diameter [5]. The SWNTs varying diameters are: those that are $< 1\ nm$, $1 < d_t < 2\ nm$ and those $> 2\ nm$. For SWNTs within $1 < d_t < 2\ nm$ diameter range, they are characterized using (10);

$$\omega_{RBM} = \frac{A}{d_t} + B \quad (10)$$

Where parameters A and B are determined experimentally. The Raman RBM frequency range covered was $120 < d_t < 250\ nm$. Typical values of A and B are 234 and 10 cm^{-1} [4].

However, for SWNTs, $d_t < 1\ nm$ diameter range, (10) does not hold due to nanotube lattice distortions leading to chirality dependence. Also, for SWNTs, $d_t > 2\ nm$ diameter range, (10) does not hold since the intensity of the RBM is so weak and is hardly observed [4]. Table I shows the approximations of the SWNTs diameters using the RBM spectra of 532 and 633 nm lasers and (10).

TABLE. I Diameter Distribution in the SWNTS.

Laser (nm)	ω cm^{-1}	A cm^{-1}	B cm^{-1}	d_t nm
532	149.9067	234	10	1.6725
	165.0505	234	10	1.5092
	183.4123	234	10	1.3494
633	135.3763	234	10	1.8664
	146.7704	234	10	1.7109
	163.5872	234	10	1.5236
	186.2358	234	10	1.3278

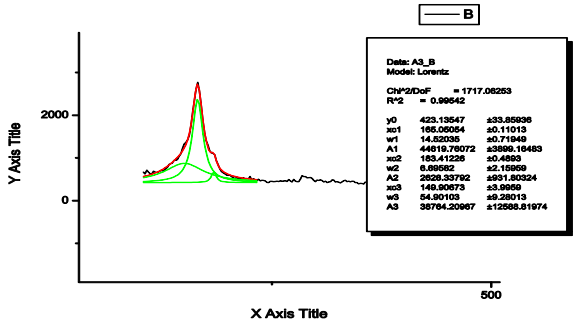

(a)

Published By:
Blue Eyes Intelligence Engineering
& Sciences Publication Pvt. Ltd.

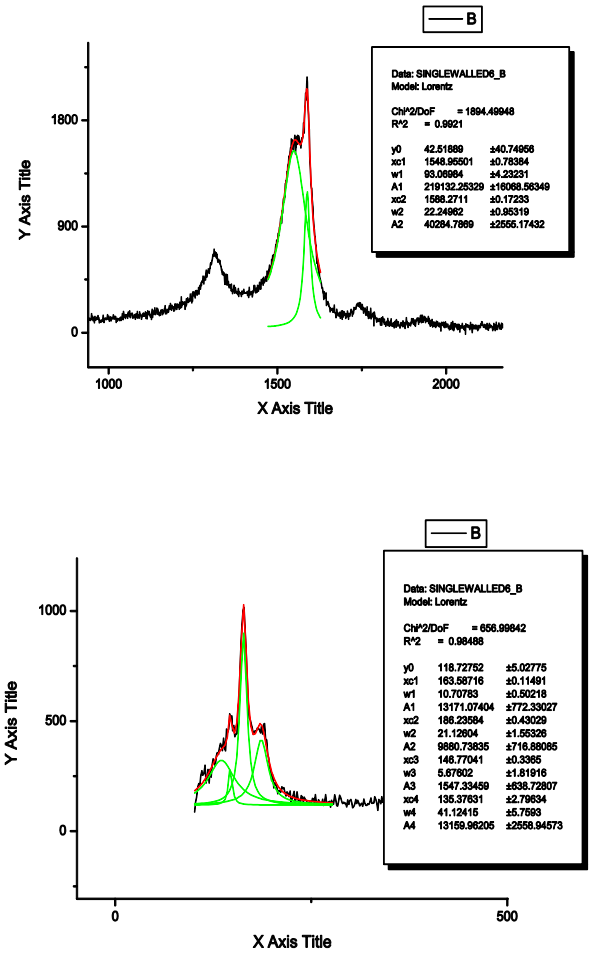

(b)

Fig. 2 Radial Breathing Mode (RBM) for SWNTs at 100-500 cm^{-1} (a) Spectrum from 532 nm laser; (b) Spectrum from 633 nm laser.

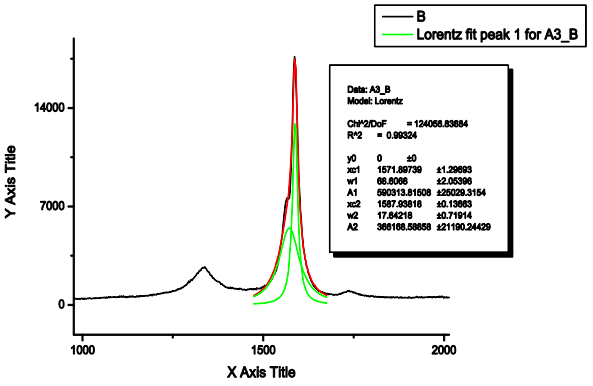

(a)

Fig. 3 Tangential mode (G-Band) for SWNTs at 1500-1700 cm^{-1} (a) Spectrum from 532 nm laser; (b) Spectrum from 633 nm laser.

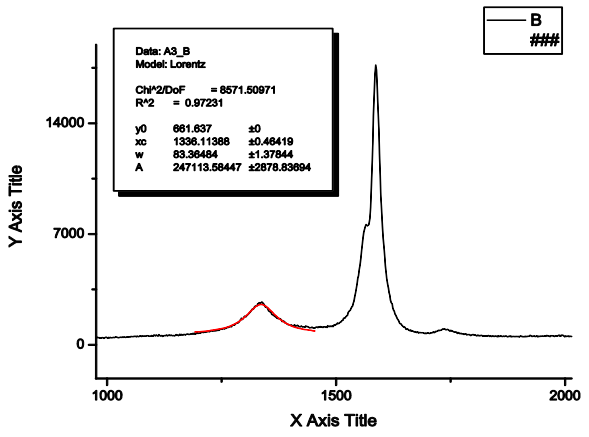

Fig. 4 Disorder-induced mode (D-Band) for SWNTs at 1200-1500 cm^{-1} from 532 nm laser

IV. CONCLUSIONS

The SWNTs investigated in this experiment had no amorphous carbon since the observed D-Band peaks were small compared with the G-peak intensity which was 5 times lager in both the 532 nm and 633 nm laser spectra.

The diameter distribution of SWNTs that were investigated in this experiments was estimated to fall between 1.3 and 1.9 nm using the RBM features of the rich Raman spectra in both 532 and 633 nm lasers as illustrated in Table I above.

ACKNOWLEDGMENT

This work was supported by Department of Mechanical and Manufacturing Engineering, Aalborg University, Denmark.

REFERENCES

1. Hollas, M.J., Modern Spectroscopy. Fourth Edition ed. 2004: John Wiley & Sons, Ltd.
2. Vandenabeele, P., Practical Raman Spectroscopy: An Introduction. 2013: John Wiley & Sons Ltd.
3. Larkin, P., Infrared and Raman Spectroscopy: Principles and Spectra Interpretation. 2011: Elsevier.
4. A. Jorio, et al., Characterizing carbon nanotube samples with resonance Raman scattering. New Journal of Physics, 2003. **5**: p. 139.1-139.17}.
5. Sergei M. Bachilo, et al., Structure-Assigned Optical Spectra of Single-Walled Carbon Nanotubes. Science, 2002. **298**: p. 2361-2366.